Dalton Transactions

Accepted Manuscript

ROYAL SOCIETY OF CHEMISTRY

www.rsc.org/dalton

Dalton Transactions

RSCPublishing

ARTICLE

Construction of Iridium and Rhodium Cyclometalated Macrocycles Based on *p*-carborane and *N,N'*-donor Bridging Ligands†

Cite this: DOI: 10.1039/x0xx00000x

DOI: 10.1039/x0xx00000x

www.rsc.org/

Xu-Yu Shen,[a] Long Zhang,[a] Yue-Jian Lin[a] and Guo-Xin Jin*[a]

Six *tetra*nuclear *half*-sandwich iridium and rhodium complexes bridged by neutral *N,N'*-donor pyridyl-imine ligands and 1,12-*di*carbadodecaborane(12)-1,12-*di*carboxylate (*p*-CDC) were controllably synthesized and fully characterized. The results revealed that the precursors, *bi*nuclear complexes $[(Cp^*M)_2\{1,4\text{-bis(2-pyridylmethyleneamino)benzene}\}Cl_2][OTf]_2$ (Cp^* = η^5-*penta*methylcyclopentadienyl, M = Ir (**2a**), Rh (**2b**)) have different preferential configurations, and *tetra*nuclear complexes $[(Cp^*M)_4\{1,4\text{-bis(2-pyridylmethyleneamino)benzene}\}_2(p\text{-CDC})_2][OTf]_4$ (M = Ir (**3a**), Rh (**3b**)), which were prepared using *mono*dentate *p*-carborane *di*carboxylate and **2a** or **2b**, showed highly twisted backbones. Likewise, homologous regular rectangular compounds $[(Cp^*M)_4\{1,4\text{-}\{(2\text{-}C_5H_4N)HC{=}N\}_2\text{-}2,3,5,6\text{-}Me_4C_6\}_2(p\text{-CDC})_2][OTf]_4$ (M = Ir (**4a**), Rh (**4b**)) and $[(Cp^*M)_4\{1,4\text{-}\{(2\text{-}C_5H_4N)HC{=}N\}_2\text{-}1,5\text{-naphthalene}\}_2(p\text{-CDC})_2][OTf]_4$ (M = Ir (**5a**), Rh (**5b**)) were obtained following a similar synthetic route, X-ray determination confirmed **4b** and **5b** have stacking channels as well.

Introduction

Since the late 1990s, the design and construction of metallomacrocycles has drawn a great deal of attention.[1] Because of their controllable shape, manageable size and specific functionalized architectures, metallomacrocycles have found applications in luminescent, electrochemical sensors, molecular sieves and catalysts.[2] Cp*M (M = Rh, Ir) *half*-sandwich metal units with a variety of advantages (modulation of redox potential, modulation of solubility, magic binding angels and etc.) have been successively used to obtain various metallomacrocycles and cages.[2c,3] Carboranes with *closo* geometries, 1,12-*di*carbadecaborane ($C_2B_{10}H_{12}$) for instance, are geometrically rigid species with an electronic structure that makes them optically transparent and redox inactive.[4] Carboranes are also icosahedral carbon-containing boron clusters that possess several material-favorable properties including rigidity, thermal stability and chemical stability.[5] *p*-CDC has been successively applied in constructing MOF materials[6] and some simple supramolecular complexes.[7] However, the coordinated centers in these materials are d-block metal ions with shorter atomic radii, such as Zn^{2+}, Co^{2+}, Cu^{2+} and Mo_2 units, thus showing a higher capability for coordination, or lanthanide ions such as Yb^{3+}, Y^{3+}, Tb^{3+}, Gd^{3+}, Sm^{3+}, Eu^{3+}, Ce^{3+} and La^{3+}. In addition, carboxyl groups in these structures are ligated to central metals through both of the conjugated oxygen atoms, or alternatively, only one carboxyl group in the *di*carboxylate ligands is bonded to the metal through one oxygen atom. The only example of carborane-containing, neutral, self-assembled twisted Pt-metallocycles was published by Stang and coworkers,[8] in which each carboxylate was bonded to Pt through one oxygen. To the best of our knowledge, no other heavier metal has been incorporated in the construction of metallomacrocycles with this carborane-based ligand. In addition, pyridyl-imine is an intriguing ligand due to its use in constructing a wealth of macrocycles,[9] helicates,[10] rotaxanes,[11] catenanes,[12] grids,[13] a Borromean link[14] and polyhedrons.[15]

Previous work from our group has focused on the preparation of metallomacrocycles based on either *di*anionic ligands or neutral ligands that were further deprotonated via C-H or B-H activation, coordinated to dimeric complexes $[Cp^*MCl_2]_2$ (M =

[a]Shanghai Key Laboratory of Molecular Catalysis and Innovative Material, *Department of Chemistry, Fudan University, Shanghai, 200433, P. R. China. E-mail: gxjin@fudan.edu.cn; Fax: (+86)-21-65643776.*

† Electronic Supplementary Information (ESI) available: CCDC No. 1004100 (**2a**), 1004102 (**2b**), 1004101 (**3a**), 1004103 (**3b**), 1022881 (**4b**) and 1018974 (**5b**) contain the supplementary crystallographic data for this paper. See http://dx.doi.org for crystallographic data in CIF or other electronic format.

Ir, Rh), then linked with neutral pyridine ligands.[16] In this paper, we chose the neutral pyridyl-imine ligand **L** (Scheme 1) (requiring no bond activation) to occupy two of three available coordination sites of the central metals. In this way, we obtained the two complexes **2a** and **2b** (Scheme 1). Though the *bi*nuclear complex [Cp*RhCl{*p*-phenylene-bis(picoline) aldamine}RhCp*Cl]$(BF_4)_2$ has been reported by M. Chandra et al.[17] with the same bridging ligand but different anion, the molecular structure was also not reported. *Bi*nuclear compounds were then controllably reacted with *p*-CDC instead of pyridine ligands. The purpose of this was to, on one hand, decrease the valence state of the macrocycles compared to those prepared using the usual neutral ligand by linking with only one oxygen atom of each carboxylate group in the carborane linker, and on the other hand, to improve the crystallinity of the resulting metallocycles by introducing a *p*-carborane linker. Fortunately, we managed to obtain *tetra*nuclear **3a** and **3b** (Scheme 2), which showed good solubility and excellent crystallinity. Meanwhile, four *tetra*nuclear macrocycles **4a**, **4b**, **5a** and **5b** were synthesized successively by replacing **L** with homologous **L**(a) and **L**(b) (Scheme 1), respectively. And their regular rectangular structures were confirmed by single-crystal X-ray crystallography.

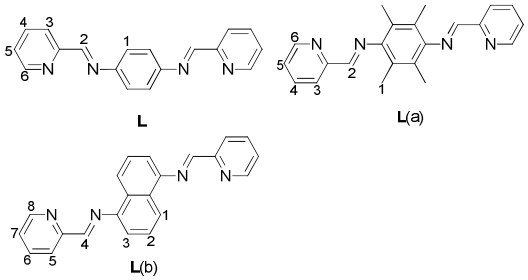

Scheme 1 Structures of neutral pyridyl-imine ligands used in this study.

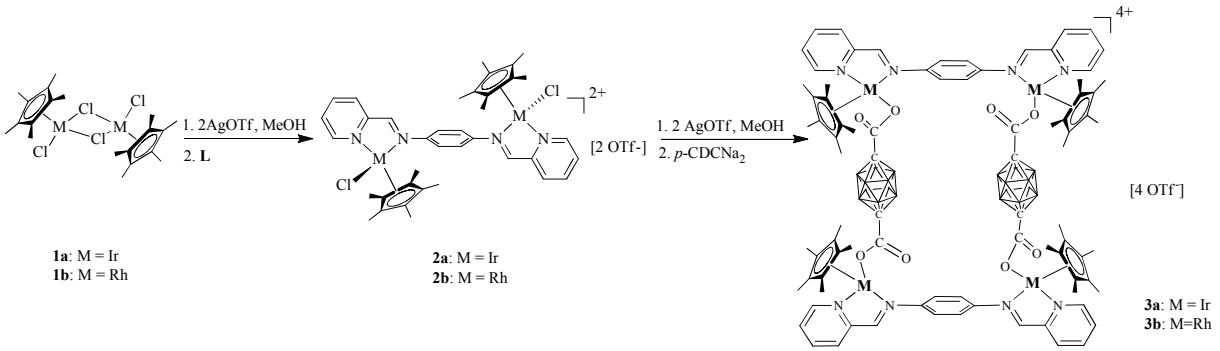

Scheme 2 Stepwise formation of *bi*nuclear and *tetra*nuclear macrocycles

Results and discussion

Synthesis and characterization

The pyridyl-imine ligand **L** was prepared simply by adding hot ethanol solutions of 1,4-*di*aminobenzene (1 equiv.) to 2-formylpyridine (2 equiv.). A yellow precipitate quickly formed, which was filtered off, recrystallized from hot ethanol, and dried in vacuo. Ligands **L**(a) and **L**(b) were prepared according to literature methods.[18] Single crystals of **2a**, **2b**, **3a**, **3b**, **4b** and **5b** were obtained by diffusion of ether into their concentrated methanol or acetonitrile (**4b**) solutions at ambient temperature. Furthermore, the structures of all the eight target products were confirmed by NMR, IR spectrum and elemental analyses.

***Bi*nuclear complexes 2a and 2b:** Two *bi*nuclear complexes were synthesized by a two-step formation strategy (Scheme 2). The IR spectra show two strong bands at 2926 cm^{-1}, 1637 cm^{-1} for **2a** and 2925 cm^{-1}, 1598 cm^{-1} for **2b** indicating the presence of Cp* and imine ligands, respectively. As the complexes can exist as diastereomers, signals for the minor diastereomer are hidden or not well resolved in the respective spectra. Therefore, we are unable to make precise assignments of the different signals. We will consider the major isomers of the metallocycles. Interesting splitting patterns of the ^{1}H NMR signals were found in **2a**, the spectrum of which indicates the presence of two kinds of Cp*Ir species in a 1:1 ratio, which means two major steric preference of the *di*nuclear compounds. Also, two sets of signals were observed in an approximate 1:1 ratio of integrated intensity at δ 9.16-9.05 (two doublets), 9.04-8.75 (two triplets), 8.47-8.02 (two multiplets), 8.00-7.98 (two singlets), 7.96-7.74 (two singlets), 7.58-7.46 (two multiplets) and 1.55-1.52 (two singlets), which were assigned to H^6, H^2, H^3, H^4, H^1, H^5 and Cp*, respectively, compared to the corresponding chemical shifts of 8.58, 8.52, 8.08, 7.68, 7.23, 7.13 of **L** and 1.5 of **1a**. Comparatively, the ^{1}H NMR spectrum of **2b** shows only one set of signals: δ 9.22 (H^6), 9.14 (H^2), 8.43 (H^3), 8.35 (H^4), 8.11 (H^1), 8.01 (H^5) and 1.42 (Cp*). All of these shifts coincide well with the corresponding chemical shifts of coordinated **2a** and **2b**. X-ray crystallographic analysis of **2a** (Figure 1a) and **2b** (Figure 1b) confirmed the different *bi*nuclear conformations.

Perspective drawings of **2a** and **2b** with partial atomic numbering scheme are given in Fig. 1. The crystal structures of **2a** and **2b** consist of *bi*nuclear units, and each iridium or rhodium atom is surrounded by one Cl atom and two N atoms from the Schiff base ligand **L**. For the central metals, angles between adjacent bonds around the metal center, such as N(1)-Ir(1)-Cl(1) (85.6(2)˚), N(2)-Ir(1)-Cl(1) (87.5(2)˚), N(1)-Rh(1)-

Cl(1) (89.4(7)˚) and N(2)-Rh(1)-Cl(1) (87.3(7)˚) are nearly 90˚. **2a** shows two types of preferential isomers: Cp* rings are almost *trans* and *cis* disposed with respect to the ligand in the ratio 1:1, which coincides well with the two sets of NMR signals observed. The distances between two iridium atoms are 8.320(1) Å (Ir(1)-Ir(2)) and 8.519(1) Å (Ir(3)-Ir(3A)). The Ir(1)-Cl(1)-Cl(2)-Ir(2) and Ir(3)-Cl(3)-Cl(3A)-Ir(3A) torsion angles are 80.1(9)˚ and 86.5(9)˚, respectively. However, the crystal structure of **2b** shows only *trans* symmetry and the Rh(1)-Rh(2) distance is 8.691(5) Å. Two Cl atoms are extended in mutually-parallel orientation.

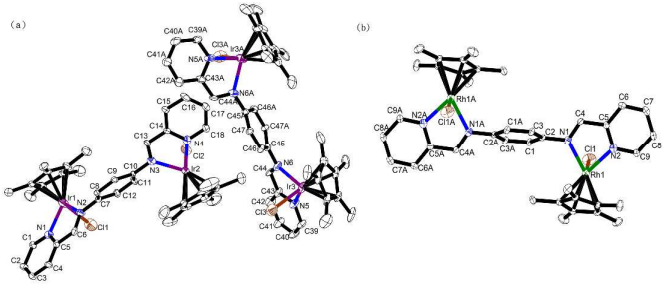

Fig. 1 Different configurations of (a) complex **2a**, and (b) **2b** with thermal ellipsoids drawn at the 30% level. All hydrogen atoms are omitted for clarity.

***Tetra*nuclear complexes 3a and 3b:** The preparation of the *tetra*nuclear complexes involved halide abstraction by AgOTf, followed by addition of a methanol solution of the linker *p*-CDC. The *tetra*nuclear compounds **3a** ($[Cp^*_4Ir_4L_2(p\text{-}CDC)_2][OTf]_4$) and **3b** ($[Cp^*_4Rh_4L_2(p\text{-}CDC)_2]$ $[OTf]_4$) were further crystallized from CH_3OH/ether. Surprisingly, high-quality single crystals suitable for X-ray determination rapidly formed over a period of 8 hours. This better crystallinity is perhaps due to the rigid and highly symmetrical properties of the carborane ligand. Likewise, IR, ^1H NMR and elemental analysis confirmed the presence of **3a** and **3b**. IR spectral bands were observed at 2617 cm^{-1} (**3a**) and 2614 cm^{-1} (**3b**) for B-H vibrations, while ^1H NMR signals were found at at 1.32-1.60 ppm (**3a**) and 1.38-1.72 ppm (**3b**). Due to the unsymmetrical coordination environment of the carborane linkers, ^{11}B NMR spectra of **3a** and **3b** both show two singlets: -13.66, -14.68 (**3a**); -13.65, -14.71 (**3b**). All of these data coincide well with the corresponding characteristic peaks of the carborane linker. IR bands at 1655 cm^{-1} (**3a**) and 1641 cm^{-1} (**3b**) also verify the presence of bound carbonyl groups. X-ray single crystal analysis of **3a** (Figure 2a) and **3b** (Figure 2d) confirm the *tetra*nuclear structures.

Perspective drawings of **3a** and **3b** with partial atomic numbering scheme are given in Fig. 2. Complexes **3a** and **3b** both crystallize in the *mono*clinic crystal system and exhibit highly distorted quadrangular structures (Figure 2a). The cations of **3a** and **3b** consist of four Cp*M corners, two neutral **L** ligands and two *di*anions *p*-CDC. Each metal center is surrounded by two N atoms and one O atom. For **3a** the O(1)-C(3)-C(4)-O(3) is torsion angle is 69.7(7)˚ and that of O(5)-C(7)-C(8)-O(7) is 73.0(7)˚, while for **3b**, the corresponding torsion angles are both 64.6(3)˚. Molecular rectangles **3a** and **3b** are twisted severely from planarity (Figure 2b); the angles between two carborane ligands are 87.1(1)˚ (**3a**) and 82.2(8)˚ (**3b**). This distortion presumably results from the flexibility of ligand **L**. The determinations indicate that one oxygen of each carboxyl group that links to the central metals. 3D packing shows that there is no channel or pore in the two materials and that the counteranions are located just outside the cycles. It is noted that the N(1)-Ir(1)-O(1) and N(2)-Ir(1)-O(1) angles are 81.2(3)˚ and 88.3(3)˚, while the distances between Ir(1)-Ir(2) and Ir(1)-Ir(3) are 8.180(7) Å and 11.471(9) Å, respectively. Similarly, the N(1)-Rh(1)-O(1) and N(2)-Rh(1)-O(1) angles are 83.1(1)˚ and 90.8(1)˚ and the distances between Rh(1)-Rh(2) and Rh(1)-Rh(3) are 8.209(9) Å and 11.432(1) Å, respectively.

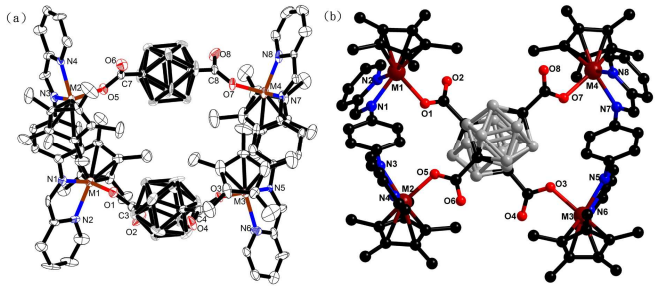

Fig. 2 Molecular structures of the *tetra*nuclear complexes **3a** (M = Ir) or **3b** (M = Rh) showing (a) thermal ellipsoids drawn at 30% level, and (b) ball and stick model viewed from the c axis. All hydrogen atoms, anions, and solvent molecules are omitted for clarity.

To further demonstrate the excellent binding properties of such carborane-containing ligands and verify the reason for the distortions, we chose another two homologous *poly*-pyridyl ligands: **L**(a) and **L**(b). Both have the same axial length as **L**. For **L**(a), four sterically-imposing methyl groups were added to the phenyl of **L**; While for **L**(b), the phenyl ring was replaced by the larger, conjugated naphthyl group. After coordination to chloride-free *half*-sandwich iridium or rhodium compounds, followed by addition of the carborane ligand, we managed to obtain four *tetra*nuclear compounds: **4a**, **4b**, **5a** and **5b**. In this way, we anticipated the twisted structures to be transferred into regular rectangles and have possible channels stacked via certain direction.

***Tetra*nuclear complexes 4a and 4b:** For **4a** and **4b**, the synthetic route involved removing all of the chloride atoms of **1a** or **1b** with AgOTf (4 equiv.), and addition of a methanol solution of **L**(a) to occupy two of three vacant coordination sites. Then, a methanol solution of linker *p*-$CDCNa_2$ was added dropwise to controllably bind with the central metals. *Tetra*nuclear **4a** ($[(Cp^*Ir)_4\{1,4\text{-}\{(2\text{-}C_5H_4N)HC{=}N\}_2\text{-}2,3,5,6\text{-}Me_4C_6\}_2(p\text{-}CDC)_2][OTf]_4$) and **4b** ($[(Cp^*Ir)_4\{1,4\text{-}\{(2\text{-}C_5H_4N)HC{=}N\}_2\text{-}2,3,5,6\text{-}Me_4C_6\}_2(p\text{-}CDC)_2][OTf]_4$) were further purified by crystallized from CH_3OH/ether. IR spectra of the two complexes exhibited characteristic bands due to the imine moiety of the ligands, along with characteristic bands corresponding to carborane ligand. The $\nu_{C=N}$ bands in the complexes shifted to higher wave numbers (1661 cm^{-1} (**4a**), 1649 cm^{-1} (**4b**)) relative to that in the free ligand (1640 cm^{-1}). The band associated with pyridyl ring appeared at about 1032 cm^{-1} (**4a**), 1031 cm^{-1} (**4b**). The shift in the position of the $\nu_{C=N}$ and pyridine ring bands suggested coordination of the metal ion through the pyridyl and imine

nitrogen atoms. Broad bands in the region 2617 cm^{-1} (**4a**) and 2614 cm^{-1} (**4b**) have been assigned to the carboxylate group of the carborane ligand. ^{11}B NMR spectra of two singlets confirmed the presence of carborane linkers in both **4a** and **4b**. The ^{1}H NMR spectrum of the free **L**(a) protons exhibited six well-resolved signals at 2.34 (H^1), 8.40 (H^2), 7.85 (H^3), 7.79 (H^4), 7.64 (H^5) and 8.65 (H^6). However, for complexes **4a** and **4b**, signals of **L**(a) exhibited a downfield shift relative to those in the free ligand upon coordination with the metal centre. Spectra of the B-H protons also exhibited an upfield shift relative to that in the carborane precursor and resonated as multiplets at δ 1.6-3.2 ppm.[7e] Elemental analyses also confirmed the expected carbon, hydrogen and nitrogen composition. All of these analyses coincide well with the corresponding characteristic peaks of the *tetra*nuclear macrocycles when they included the more sterically-hindered poly-pyridyl ligand **L**(a).

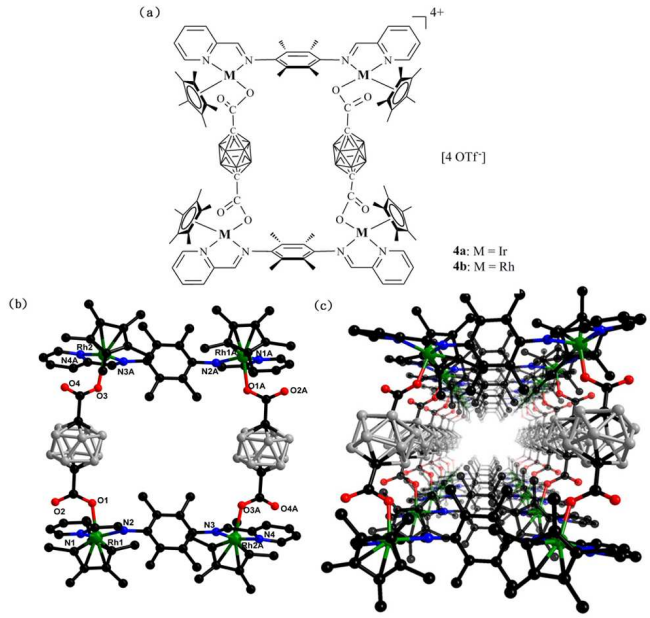

Fig. 3 (a) Sketch of **4a** (M = Ir) and **4b** (M = Rh)**,** molecular structures of **4b** showing (b) ball and stick model, and (c) crystal structure packing viewed from the x axis, All hydrogen atoms, anions, and solvent molecules are omitted for clarity.

Perspective crystal structural sketch of 4**b** is given in Fig. 3a. Complex **4b** crystallizes in the triclinic crystal system and exhibits regular rectangular structure (Figure 3b). Two Cp* rings are almost *cis* disposed. Both O(1)-C(2)-C(4)-O(3) and O(1A)-C(2A)-C(4A)-O(3A) are less twisted with the torsion angle 55.64˚. Carborane groups and phenyl groups are parallel. Compared with **3a** or **3b**, the reason for the structural modification is that the four methyl groups block the flexibility of the phenyl group, and two pyridyl groups are almost parallel consequently. 3D packing shows the formation of channels viewed from the x axis (Fig. 3c). The anions OTf^- locate just between the adjacent cycles. And there exists two kinds of weak driving forces, C-H···O between Cp* ring and OTf^- , B-H···F between OTf^- and carborane of another cycle, both of which result in the construction of layered channels. All the solvent molecules are distributed around the cycles. It is noted that the N(1)-Rh(1)-O(1) and N(2)-Rh(1)-O(1) angles are 80.345(6)˚ and 83.573(8)˚, while the distances between Rh(1)-Rh(2) and Rh(1)-Rh(2A) are 11.3195(8) Å and 8.4683(6) Å, respectively.

***Tetra*nuclear complexes 5a and 5b:** For **5a** and **5b**, the synthetic route analogous to that of **4a** and **4b**. Solutions of *tetra*nuclear compounds **5a** ($[(Cp^*Ir)_4\{1,4\text{-}\{(2\text{-}C_5H_4N)HC{=}N\}_2\text{-}1,5\text{-naphthalene}\}_2(p\text{-}CDC)_2][OTf]_4$) and **5b** ($[(Cp^*Rh)_4\{1,4\text{-}\{(2\text{-}C_5H_4N)HC{=}N\}_2\text{-}1,5\text{-naphthalene}\}_2(p\text{-}CDC)_2][OTf]_4$) were further crystallized from CH_3OH/ether. Likewise, the IR spectra of coordinated **5a** and **5b** showed approximately the same features as their counterparts **4a** and **4b**. Similarly, ^{11}B NMR spectra showed two singlets for **5a** and **5b**. The ^{1}H NMR spectrum of the free **L**(b) protons exhibited eight well-resolved signals at 8.21 (H^1), 7.43 (H^2), 7.44 (H^3), 8.40 (H^4), 7.85 (H^5), 7.79 (H^6), and 7.64 (H^7) and 8.65 (H^8). The ^{1}H NMR spectra of the complexes **5a** and **5b** followed the general trends observed in the proton NMR spectra of the **L**(b) and carborane ligands. The position and integrated intensity of different signals matched the formulation of the complexes **5a** and **5b** well. Elemental analysis also verified the chemical compositions. The above analytical and spectral data are consistent with our formulation of the complexes.

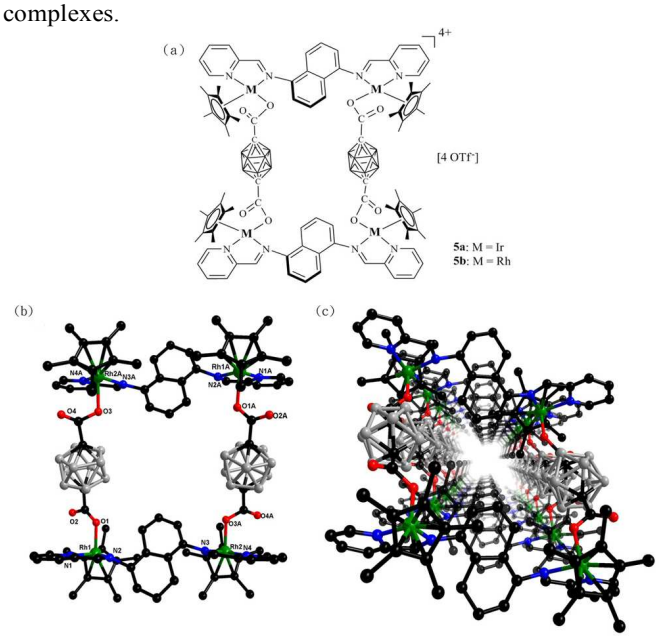

Fig. 4 (a) Sketch of **5a** (M = Ir) and **5b** (M = Rh)**,** molecular structures of **5b** showing (b) ball and stick model, and (c) crystal structure packing viewed from the x axis, All hydrogen atoms, anions, and solvent molecules are omitted for clarity.

Perspective crystal structural sketch of 5**b** is given in Fig. 4a. Complex **5b** crystallizes in the triclinic crystal system and exhibits approximate regular rectangular structure (Figure 4b). Two Cp* rings are almost *cis* disposed and two naphthyl groups are fully parallel. O(1)-C(3)-C(4)-O(3) and O(1A)-C(3A)-C(4A)-O(3A) are more twisted ever with the torsion angle 75.616˚, two carborane groups are also parallel, both of which

further demonstrate the torsion of the carboxylate groups does not lead to the highly twisted cycles. Comparatively, bulky naphthyl group are much less flexible than phenyl group, and two pyridyl groups are almost parallel consequently. Therefore, the flexibility of the **L** really results in the distortion of **3a** and **3b**. 3D packing shows the formation of channels viewed from the x axis (Fig. 4c). Weak driving force, C-H···O between Cp* ring and carboxyl group of neighboring cycle, contributes to the construction of layered channels. All the solvent molecules and counteranions are distributed outside of the cycles. It is noted that the N(1)-Rh(1)-O(1) and N(2)-Rh(1)-O(1) angles are 80.83(9)° and 78.75(1)°, while the distances between Rh(1)-Rh(2) and Rh(1)-Rh(2A) are 8.7627(17) Å and 11.4992(18) Å, respectively.

Conclusions

In conclusion, a series of *bi*- and *tetra*nuclear *half*-sandwich iridium and rhodium complexes have been synthesized and characterized. The *bi*nuclear structures indicate two steric isomers for iridium, but only one isomer for rhodium. The successful synthesis of *tetra*nuclear carborane-based complexes offers us an excellent *mono*-dentate-bound carborane *di*carboxylate linker to rationally form macrocycles with iridium and rhodium that show better crystallinity, solubility and a number of potential applications, many of which may have packed channels in certain direction.

Experimental section

General Details. All manipulations were performed under an atmosphere of nitrogen using standard Schlenk techniques. The starting materials $[Cp^*IrCl(\mu\text{-}Cl)]_2$ and $[Cp^*RhCl(\mu\text{-}Cl)]_2$ were prepared according to literature methods.[19] The proligand 1,12-*di*carbadodecaborane(12)-1,12-*di*carboxylic acid was also synthesized according to literature methods.[6e] Its sodium salt was prepared by mixing the *p*-$CDCH_2$ with sodium methylate in MeOH at ambient temperature. Other chemicals were obtained commercially and used without further purification. Elemental analyses were performed on an Elementar III Vario EI analyzer. $^1H/^{11}B$ NMR (400 MHz) spectra were recorded on a Bruker VAVCE-DMX 400 Spectrometer in $[D_6]$-DMSO solution.

X-ray Crystal Structure Determinations. All single crystals were characterized at low temperature. Data were collected on a CCD-Bruker SMART APEX system. All unit cell determinations and intensity data were performed with graphite *mono*chromatic Mo Kα radiation (λ = 0.71073 Å). All the data were collected at -100 ºC using the ω-scan technique. The structures were solved by direct methods, using Fourier techniques, and refined on F^2 by a full-matrix least-squares method. All calculations were carried out with the SHELXTL program. In asymmetric unit of **2a**, there was disordered solvent molecule (one dichloromethane) which could not be restrained properly. Therefore, SQUEEZE algorithm was used to omit it. 18 ISOR and 1 DFIX instructions were used to restrain the Cp* fragments and solvents so that there were 109 restraints in the data. For **3a**, there were disordered solvents (three methanol and one diethyl ether molecules) which could not be restrained properly. SQUEEZE algorithm were used to omit them. One OTf^- anion was disordered and it was divided into two parts (72:28). C(85), C(86) and C(88) were refined isotropically because NPD and other non-hydrogen atoms were refined anisotropically. 36 DFIX and 26 ISOR instructions were used to restrain anions and Cp* ligands so that there were 192 restraints in the data. Hydrogen atoms were put in calculated positions but hydrogen atoms of water molecules could not be found. For **3b**, there were disordered solvents (one methanol and one water molecules). SQUEEZE algorithm was used to omit them. O(6), O(8), O(13), F(3), F(5), F(6), C(43) and C(45) were refined isotropically because NPD and other non-hydrogen atoms were refined anisotropically. 39 DFIX and 17 ISOR instructions were used to restrain anions so that there were 141 restraints in the data. For **4b**, there were disordered solvents (three methanol and two water molecules) which could not be restrained properly. SQUEEZE algorithm was used to omit them. 14 ISOR, 1 DELU and 16 DFIX instructions were used to restrain anions, solvents and Cp* fragments so that there were 101 restraints in the data. Hydrogen of water molecules could not be found and others were put in calculated positions. For **5b**, there were disordered anions and solvent (two triflate anions and one methanol molecule) which could not be restrained properly. SQUEEZE algorithm was used to omit them. The naphthalene ring was disordered and it was divided into two parts (70:30). 25 ISOR, 1 FLAT, 2 DELU and 23 DFIX instructions were used to restrain solvents and ligands so that there were 179 restraints in the data. Hydrogen of methanol molecules could not be found and others were put in calculated positions. A summary of the crystallographic data are given in Table 1

Synthesis of complexes 2a and 2b. To a solution of $[Cp^*IrCl(\mu\text{-}Cl)]_2$ (**1a** 40 mg, 0.05 mmol) or $[Cp^*RhCl(\mu\text{-}Cl)]_2$ (**1b** 31.1 mg, 0.05 mmol) in MeOH (15 mL), AgOTf (25.7 mg, 0.10 mmol) was added and the mixture was sheltered from light. After stirring at room temperature for 4 h, the silver salt precipitate was removed by filtering under nitrogen atmosphere. Powder of **L** (14.3 mg, 0.05 mmol) was added into the remaining solution and stirred vigorously for 12 h. Later, the solution was concentrated on a rotary evaporator to 3 mL and extracted with diethyl ether (20 mL). The orange products were separated by centrifuge and further dried under vacuum: **2a**, 45.5 mg, 69.9%; **2b**, 42.8 mg, 76.3%.

Data for complex 2a: Anal. Calcd for $C_{40}H_{44}Cl_2F_6Ir_2N_4O_6S_2$: C 36.67; H 3.38; N 4.28. Found: C 36.49; H 3.38; N 4.25. ^1H NMR (400 MHz, DMSO-D_6): 9.14 (2H, d, H^6), 9.07 (2H, d, H^6), 9.02 (2H, t, H^2), 8.80 (2H, t, H^2), 8.43 (2H, m, H^3), 8.33 (2H, m, H^3), 8.00 (2H, d, H^4), 7.99 (2H, d, H^4), 7.56 (4H, m, H^1), 7.49 (4H, m, H^1), 6.80 (2H, t, H^5), 6.72 (2H, t, H^5), 1.55 (30H, s, Cp*), 1.53 (30H, s, Cp*). IR (KBr, cm^{-1}): 2926 (s), 1497 (s), 1385 (s), 1258 (w), 1161 (s), 1031 (s), 639 (s), 518 (s).

Data for complex 2b: Anal. Calcd for $C_{40}H_{44}Cl_2F_6N_4O_6Rh_2S_2$: C 42.46; H 3.92; N 4.95. Found: C, 42.63; H, 3.93; N, 4.97. ^{1}H NMR (400 MHz, DMSO-D_6): 9.22 (2H, d, H^6), 9.14 (2H, s, H^2), 8.43 (2H, t, H^3), 8.35 (2H, d, H^4), 8.11(4H, s, H^1), 8.01(2H, H^5), 1.42(30H, s, Cp*). IR (KBr, cm^{-1}): 2925 (s), 1499 (s), 1378 (s), 1259 (w), 1170 (s), 1029 (s), 638 (s), 517 (s).

Synthesis of complexes 3a and 3b. To a solution of **2a** (65.1 mg, 0.05 mmol) or **2b** (56.1 mg, 0.05 mmol) in MeOH (15 mL), AgOTf (25.7 mg, 0.10 mmol) was added and the mixture was sheltered from light. After stirring at room temperature for 4 h, the silver salt precipitate was removed by filtering. Powder of *p*-$CDCNa_2$ (13.8 mg, 0.05 mmol) was then added dropwise. After stirring for 12 h, the solution was dried on a rotary evaporator, and MeOH (3 mL) and diethyl ether (20 mL) were sequentially added to the concentrate. Red solids were separated by centrifuge and further dried under vacuum: **3a**, 103.6 mg, 71.0%; **3b**, 97.8 mg, 76.4%.

Data for complex 3a: Anal. Calcd for $C_{88}H_{108}B_{20}F_{12}Ir_4N_8O_{20}S_4$: C, 35.96; H, 3.70; N, 3.81. Found: C, 35.88; H, 3.69; N, 3.80. ^{1}H NMR (400 MHz, DMSO-D_6): 9.56 (4H, s, H^6), 9.20 (4H, d, H^2), 8.43 (4H, m, H^3), 8.03 (4H, m, H^4), 7.97 (12H, m, H^5 and H^1), 1.24-1.60 (20H, m, B-H), 1.39 (60H, s, Cp*). ^{11}B NMR (160 MHz, DMSO-D_6): -13.65(10H, s, *p*-CDC^{2-}), -14.71(10H, s, *p*-CDC^{2-}). IR (KBr, cm^{-1}): 2924 (s), 2617 (s), 1655 (w), 1499 (s), 1258 (s), 1226 (s), 1163 (s), 1032 (s), 788 (w), 640 (s), 575 (s), 518 (s).

Data for complex 3b: Anal. Calcd for $C_{88}H_{108}B_{20}F_{12}Rh_4N_8O_{20}S_4$: C, 40.94; H, 4.22; N, 4.34. Found: C, 40.94; H, 4.24; N, 4.35. ^{1}H NMR (400 MHz, DMSO-D_6): 9.15 (4H, d, H^6), 9.08(4H, d, H^2), 8.44 (4H, m, H^3), 8.05 (4H, m, H^4), 8.00 (4H, s, H^5), 7.99 (8H, s, H^1), 1.38-1.72 (20H, m, B-H), 1.55 (60H, s, Cp*). ^{11}B NMR (160 MHz, DMSO-D_6): -13.66 (10H, s, *p*-CDC^{2-}), -14.68 (10H, s, *p*-CDC^{2-}). IR (KBr, cm^{-1}): 2924 (s), 2614 (s), 1641 (w), 1498 (s), 1259 (s), 1225 (s), 1161 (s), 1031 (s), 785 (w), 639 (s), 574 (s), 517 (s).

Synthesis of complexes 4a, 4b, 5a and 5b. To a solution of **1a** (40.0 mg, 0.05 mmol) or **1b** (31.1 mg, 0.05 mmol) in MeOH (15 mL), AgOTf (51.4 mg, 0.20 mmol) was added and the mixture was sheltered from light. After stirring at room temperature for 4 h, the silver salt precipitate was removed by filtering, powder of **L**(a) or **L**(b) was added, then with the powder of *p*-$CDCNa_2$ (13.8 mg, 0.05 mmol) over 5 hours. After stirring for another 12 h, the solution was dried on a rotary evaporator, and MeOH (3 mL) and diethyl ether (20 mL) were sequentially added to the concentrate: **4a** (red), 107.8 mg, 70.5%; **4b** (yellow), 101.5 mg, 75.1%; **5a** (brown), 105.0 mg, 69%; **5b** (yellow), 86.9 mg, 65%.

Data for complex 4a: Anal. Calcd for $C_{96}H_{132}B_{20}F_{12}Ir_4N_8O_{20}S_4$: C, 37.69; H, 4.35; N, 3.66. Found: C, 37.54; H, 4.33; N, 3.69. ^{1}H NMR (400 MHz, DMSO-D_6): 9.63 (4H, d, H^6), 9.12 (4H, m, H^2), 8.45 (4H, m, H^3), 8.41 (4H, dd, H^4), 7.95 (4H, t, H^5), 2.08 (24H, m, H^1), 1.20-1.58 (20H, m, B-H), 1.39 (60H, s, Cp*). ^{11}B NMR (160 MHz, DMSO-D_6): -14.10 (10H, s, *p*-CDC^{2-}), -14.98 (10H, s, *p*-CDC^{2-}). IR (KBr, cm^{-1}): 2925 (s), 2617 (s), 1661 (w), 1454 (s), 1386 (s), 1228 (s), 1163 (s), 1032 (s), 789 (w), 640 (s), 574 (s), 517 (s).

Data for complex 4b: Anal. Calcd for $C_{96}H_{132}B_{20}F_{12}Rh_4N_8O_{20}S_4$: C, 42.67; H, 4.92; N, 4.15. Found: C, 42.59; H, 4.95; N, 4.14. ^{1}H NMR (400 MHz, DMSO-D_6): 9.16 (4H, d, H^6), 8.80 (4H, m, H^2), 8.40 (4H, m, H^3), 8.26 (4H, dd, H^3), 7.95 (4H, t, H^4), 2.08 (24H, m, H^1), 1.20-1.57 (20H, m, B-H), 1.39 (60H, s, Cp*). ^{11}B NMR (160 MHz, DMSO-D_6): -14.13 (10H, s, *p*-CDC^{2-}), -14.97 (10H, s, *p*-CDC^{2-}). IR (KBr, cm^{-1}): 2926 (s), 2614 (s), 1649 (w), 1455 (s), 1387 (s), 1227 (s), 1161 (s), 1031 (s), 786 (w), 639 (s), 574 (s), 517 (s).

Data for complex 5a: Anal. Calcd for $C_{96}H_{116}B_{20}F_{12}Ir_4N_8O_{20}S_4$: C, 37.89; H, 3.84; N, 3.68. Found: C, 37.83; H, 3.86; N, 3.66. ^{1}H NMR (400 MHz, DMSO-D_6): 9.74 (4H, d,H^8), 9.61 (4H, d, H^4), 9.07 (4H, s, H^1), 8.46 (4H, m, H^5), 8.40 (4H, t, H^6), 7.97 (4H, t, H^7), 7.85 (4H, t, H^3), 7.60 (4H, d, H^2) 1.44-1.50 (20H, m, B-H), 1.32 (60H, s, Cp*). ^{11}B NMR (160 MHz, DMSO-D_6): -13.97(10H, s, *p*-CDC^{2-}), -14.96 (10H, s, *p*-CDC^{2-}). IR (KBr, cm^{-1}): 3085 (s), 2615 (s), 1663 (w), 1592 (s), 1566 (s), 1477 (s), 1161 (s), 1031 (s), 787 (w), 639 (s), 574 (s), 517 (s).

Data for complex 5b: Anal. Calcd for $C_{96}H_{116}B_{20}F_{12}Rh_4N_8O_{20}S_4$: C, 42.85; H, 4.17; N, 4.35. Found: C, 42.93; H, 4.14; N, 4.32. ^{1}H NMR (400 MHz, DMSO-D_6): 9.24 (4H, d, H^8), 9.09 (4H, d, H^4), 8.55 (4H, m, H^1), 8.42 (4H, t, H^5), 8.00 (4H, t, H^6), 7.85 (4H, t, H^7), 7.78 (4H, t, H^3), 7.68 (4H, d, H^2) 1.27-1.37 (20H, m, B-H), 1.21 (60H, s, Cp*). ^{11}B NMR (160 MHz, DMSO-D_6): -13.99 (10H, s, *p*-CDC^{2-}), -14.96 (10H, s, *p*-CDC^{2-}). IR (KBr, cm^{-1}): 3082 (s), 2614 (s), 1644 (w), 1594 (s), 1568 (s), 1478 (s), 1258 (s), 1161 (s), 1031 (s), 785 (w), 639 (s), 574 (s), 517 (s).

Table 1. Crystallographic Data and Structure Refinement Parameters for **2a**, **2b**, **3a**, **3b**, **4b** and **5b**

	2a	2b	3a	3b	4b	5b
empirical formula	$C_{138}H_{156}Cl_{14}F_{18}Ir_6N_{12}O_{18}S_6$	$C_{40}H_{44}Cl_2F_6N_4O_6Rh_2S_2$	$C_{95}H_{138}B_{20}F_{12}Ir_4N_8O_{28}S_4$	$C_{90}H_{120}B_{20}F_{12}N_8O_{24}Rh_4S_4$	$C_{102}H_{164}B_{20}F_{12}N_8O_{34}Rh_4S_4$	$C_{100}H_{128}B_{20}F_{12}N_8O_{24}Rh_4S_4$
fw	4454.60	1131.63	3181.37	2682.01	3030.48	2810.18
crystal system	Monoclinic	Triclinic	Monoclinic	Monoclinic	Monoclinic	Triclinic
space group	*C2/c*	$P\bar{1}$	*P2(1)/c*	*C2/c*	*P2(1)/n*	$P\bar{1}$
a (Å)	23.249(3)	8.9099(7)	17.7262(18)	18.5981(19)	13.1486(14)	11.849(3)
b (Å)	20.772(3)	10.7092(8)	25.171(3)	40.947(5)	18.488(2)	16.951(4)
c (Å)	35.211(5)	11.8825(9)	27.215(3)	16.9617(18)	30.333(3)	17.367(4)
α (deg)	90	90.0310(10)	90	90	90	74.651(3)
β (deg)	108.444(2)	95.8710(10)	95.667(2)	104.947(2)	102.403(2)	79.539(3)
γ (deg)	90	91.7070(10)	90	90	90	88.193(3)

volume (Å^3)	16131(4)	1127.35(15)	12083(2)	12480(2)	7201.7(13)	3307.3(12)
Dc (g•cm^{-3})	1.834	1.667	1.749	1.427	1.398	1.411
μ(Mo Kα) (mm^{-1})	5.324	1.017	4.552	0.669	0.594	0.635
F(000)	8680	570	6272	5440	3112	1428
θ range (deg)	1.219-27.499	1.723-27.526	1.154 -25.010	0.995-26.010	1.587-26.999	1.236 - 26.000
limiting indices	-25,30;24,26;-45,45	-11,11;-10,13;-13,15	-17,21; -29,29; -32,32	-22,22;-50,50;-20,11	-16,12; -23, 23; -38, 38	-13,14; -20, 18; -21, 21
Reflections/unique [*R(int)*]	57266/18388[0.0637]	8328/5089[0.0160]	72543/21257 [0.1155]	39953/12258 [0.0630]	15616/49815[0.0776]	12844/21411[0.0487]
completeness to *θ* (deg)	99.4 %	97.8 %	97.2 %	99.7 %	99.3 %	98.7 %
data/restraints/params	18 388/109/933	5089 /0 /285	21257 /192 /1495	12258/141/745	15616 / 101 / 771	12844/173/707
goodness-of-fit on F^2	1.061	1.084	0.911	1.078	1.015	0.976
$R_1{}^a$,$wR_2{}^a$ [I > 2σ(I)]	0.0709, 0.1684	0.0347,0.0865	0.0633, 0.1457	0.0870, 0.2488	0.0998, 0.2777	0.0968, 0.2715
R_1, wR_2 (all data)	0.1003, 0.1803	0.0421,0.1017	0.1265, 0.1705	0.1184,0.2797	0.1591, 0.3085	0.1576, 0.3098

Acknowledgment

This work was supported by the National Science Foundation of China (91122017, 21374019), the Shanghai Science and Technology Committee (13JC1400600, 13DZ2275200) and the Program for Changjiang Scholars and Innovative Research Team in University (IRT1117).

Notes and references

1 (a) B. Olenyuk and P. J. Stang, *Acc. Chem. Res.,* 1997, **30**, 502-518. (b) S. Leininger, B. Olenyuk and P. J. Stang, *Chem. Rev.,* 2000, **100**, 853-907. (c) M. Fujita, M. Tominaga, A. Hori and B. Therrien, *Acc. Chem. Res.,* 2005, **38**, 369-378. (d) B. J. Holliday and C. A. Mirkin, *Angew. Chem., Int. Ed.,* 2001, **40**, 2022-2043. (e) A. Rit, T. Pape and F. E. Hahn, *J. Am. Chem. Soc.,* 2010, **132**, 4572-4573. (f) F. E. Hahn and M. C. Jahanke, *Angew. Chem., Int. Ed.,* 2008, **47**, 3122-3172. (g) F. A. Cotton, C. Lin and C. A. Murillo, *Acc. Chem. Res.,* 2001, **34**, 759-771. (h) M. Fujita, K. Umemoto, M. Yoshizawa, N. Fujita, T. Kusukawa and K. Biradha, *Chem. Commun.,* 2001, 509-518. (i) T. R. Cook, V. Vajpayee, M. H. Lee, P. J. Stang and K.-W Chi, *Acc. Chem. Res.,* 2013, **46**, 2464-2474. (j) T. R. Cook, Y. R. Zheng and P. J. Stang, *Chem. Rev.,* 2012, **113**, 734-777. (k) C. A. Housecroft, *Dalton Trans.,* 2014, **43**, 6594-6604.

2 (a) F. Würthner, C. C. You and C. R. Saha-Möller, *Chem. Soc. Rev.,* 2004, **33**, 133-146. (b) J. L. Boyer, M. L. Kuhlman and T. B. Rauchfuss, *Acc. Chem. Res.,* 2007, **40**, 233-242. (c) K. Severin, *Chem. Commun.,* 2006, 3859-3867. (d) C. H. M. Amijs, G. P. M. van Klink and G. van Koten, *Dalton Trans.,* 2006, 308-327. (e) P. Thanasekaran, R. T. Liao, Y. H. Liu, T. Rajendran, S. Rajagopal and K. L. Lu, *Coord. Chem. Rev.,* 2005, **249**, 1085-1110. (f) A. Kumar, S. S. Sun, A. J. Lees, *Coord. Chem. Rev.,* 2008, **252**, 922-939. (g) T. Jacobs, G. O. Lloyd, J. Gertenbach and K. K. Müller-Nedebock, *Angew. Chem. Int. Ed.*, 2012, **51**, 4913-4916. (h) F. Li, J. K. Clegg, L. Goux-Capes, G. Chastanet, D. M. D'Alessandro, J. Létard and C. J. Kepert, *Angew. Chem. Int. Ed.,* 2011, **50**, 2820-2823. (i) S. Perera, X. P. Li, M. Soler, A. Schultz and C. Wesdemiotis, *Angew. Chem. Int. Ed.,* 2010, **49**, 6539-6544. (j) Y. T. Chan, X. P., J. Yu, G. A. Carri, C. N. Moorefield, G. R. Newkome and C. Wesdemiotis, *J. Am. Chem. Soc.,* 2011, **133**, 11967-11976.

3 (a) S. Liu, G. L. Wang and G. X. Jin, *Dalton Trans.,* 2008, 425-432. (b) Y. F. Han, W. G. Jia, W. B. Yu and G. X. Jin, *Chem. Soc. Rev.,* 2009, **38**, 3419-3434. (c) T. B. Rauchfuss and S. Kay, *Organic Nanostructures,* 2008, 179-203. (d) N. P. E. Barry and P. J. Sadler, *Chem. Soc. Rev.,* 2012, **41**, 3264-3279. (e) J. K. Liu, X. F. Wu, J. A. Iggo and J. L. Xiao, *Coord. Chem. Rev.,* 2008, **252**, 782-809. (f) Y. F. Han and G. X. Jin, *Chem. Soc. Rev.,* 2014, **43**, 2799-2823.

4 (a) D. Hablot, A. Sutter, P. Retailleau and R. Ziessel, *Chem. Eur. J.,* 2012, **18**, 1890-1895. (b) V. I. Bregadze, *Chem. Rev.,* 1992, **92**, 209-223. (c) R. E. Williams, *Chem. Rev.,* 1992, **92**, 177-207. (d) L. A. Leites, *Chem. Rev.,* 1992, **92**, 279-323.

5 M. F. Hawthorne, *Advances in Boron Chemistry*; Special Publication No. 201; Royal Society of Chemistry: London, 1997; Vol. 82, p 261.

6 (a) Y. S. Bae, O. K. Farha, A. M. Spokoyny, C. A. Mirkin, J. T. Hupp and R. Q Snurr, *Chem. Commun.,* 2008, 4135-4137. (b) O. K. Farha, A. M. Spokoyny, K. L. Mulfort, S. Galli, J. T. Hupp and C. A. Mirkin, *Small,* 2009, **5**, 1727-1731. (c) H. Li, M. Eddaoudi, T. L. Groy and O. M. Yaghi, *J. Am. Chem. Soc.,* 1998, **120**, 8571-8572. (d) S. L. Huang, Y. J. Lin, W. B. Yu and G. X. Jin *ChemPlusChem,* 2012, **77**, 141-147. (e) O. K. Farha, A. M. Spokoyny, K. L. Mulfort, M. F. Hawthorne, C. A. Mirkin and J. T. Hupp, *J. Am. Chem. Soc.,* 2007, **129**, 12680-12681.

7 F. A. Cotton, J. P. Donahue, C. Lin and C. A. Murillo, *Inorg. Chem.,* 2001, **40**, 1234-1244.

8 N. Das; P. J. Stang, A. M. Arif and C. F. Campana, *J. Org. Chem.,* 2005, **70**, 10440-10446.

9 (a) M. J. MacLachlan, *Pure Appl. Chem.,* 2006, **78**, 873-888. (b) L. L. Schafer, J. R. Nitschke, S. S. H. Mao, F. Q. Liu, G. Harder, M. Haufe and T. D. Tilley, *Chem. Eur. J.,* 2002, **8**, 74-83.

10 (a) K. Hiratani, *New J. Chem.,* 2003, **27**, 886-889. (b) L. J. Childs, N. W. Alcock and M. J. Hannon, *Angew. Chem., Int. Ed.,* 2002, **41**, 4244-4247. (c) J. Hamblin, L. J. Childs, N. W. Alcock and M. J. Hannon, *J. Chem. Soc., Dalton Trans.* 2002, 164-169. (d) J. R. Nitschke, D. Schultz, G. Bernardinelli, D. Gérard, *J. Am. Chem. Soc.,* 2004, **126**, 16538-16543.

11 L. Hogg, D. A. Leigh, P. J. Lusby, A. Morelli, S. Parsons and J. K. Y. Wong, *Angew. Chem., Int. Ed.,* 2004, **43**, 1218-1221.

12 D. A. Leigh, P. J. Lusby, S. J. Teat, A. J. Wilson and J. K. Y. Wong, *Angew. Chem., Int. Ed.,* 2001, **40**, 1538-1543.

13 (a) J. R. Nitschke and J. M. Lehn, *Proc. Nat. Acad. Sci. U.S.A.* 2003, **100**, 11970-11974. (b) J. R. Nitschke, M. Hutin and G. Bernardinelli, *Angew. Chem., Int. Ed.*, 2004, **43**, 6724-6727. (c) S. Brooker, S. J. Hay and P. G. A Plieger, *Angew. Chem., Int. Ed.,* 2000, **39**, 1968-1970.

14 K. S. Chichak, S. J. Cantrill, A. R. Pease, S.-H. Chiu, G. W. V. Cave, J. L. Atwood and J. F. Stoddart, *Science,* 2004, **304**, 1308-1312.

15 (a) J. R. Nitschke, *Acc. Chem. Res.,* 2007, **40**, 103-112. (b) R. A. Bilbeisi, T. K. Ronson and J. R. Nitschke, *Angew. Chem. Int. Ed.,* 2013, **52**, 9027-9030 (c) C. Browne, S. Brenet, J. K. Clegg and J. R. Nitschke, *Angew. Chem. Int. Ed.,* 2013, **52**, 1944-1948.

16 (a) W. B. Yu, Y. F. Han, Y. J. Lin and G. X. Jin, *Organometallics,* 2011, **30**, 3090-3095. (b) W. B. Yu, Y. F. Han, Y. J. Lin and G. X Jin, *Organometallics,* 2010, **29**, 2827-2830. (c) T. Wu, L. H. Weng and G. X. Jin, *Chem. Commun.,* 2012, **48**, 4435-4437. (d) S. L. Huang, Y. J. Lin, T. S. Andy Hor and G. X. Jin, *J. Am. Chem. Soc.,* 2013, **135**, 8125-8128. (e) Z. J. Yao, W. B. Yu, Y. J. Lin, S. L. Huang, Z. H. Li and G. X. Jin, *J. Am. Chem. Soc.,* 2014, **136**, 2825-2832. (f) H. Li, Y. F. Han, Y. J. Lin, Z. W. Guo and G. X. Jin, *J. Am. Chem. Soc.,* 2014, 136, 2982-2985.

17 M. Chandra, A. N. Sahay, S. M. Mobin and D. S. Pandey, *J. Organomet. Chem.,* 2002, **658**, 43-49.

18 (a) J. D.A. Pelletier, J. Fawcett, K. Singh and G. A. Solan**,** *J. Org. Chem.,* 2008, **693**, 2723-2731. (b) A. K. Mandal, M. Suresh, P. Das, E. Suresh, M. Baidya, S. K. Ghosh, and A. Das, *Org. Lett.,* 2012, **14**, 2980-2983.

19 C. White, A. Yates and P. M. Maitlis, *Inorg. Synth.,* 1992, **29**, 228-234.

Graphical Abstract

1. Color Graphic

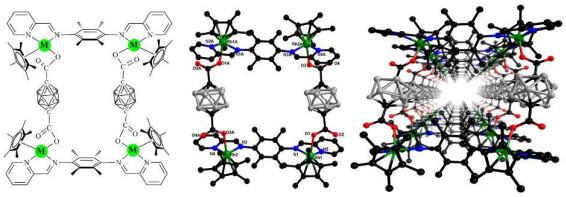

2. Text （no more than 20 words）

Construction of shape controllable macrocycles with stacking channels from *p*-carborane and pyridine-imine ligands